This work will be published in the European Journal of Mechanics-A/Solids.
Further details are available at the URL:
http://dx.doi.org/10.1016/j.euromechsol.2009.10.011

Electro-elastostatic analysis of multiple cracks in an infinitely long piezoelectric strip: a hypersingular integral approach

L. Athanasius, W. T. Ang* and I. Sridhar
School of Mechanical and Aerospace Engineering
Nanyang Technological University
Republic of Singapore

Abstract

The problem of an arbitrary number of arbitrarily oriented straight cracks in an infinitely long piezoelectric strip is considered here. The cracks are acted by suitably prescribed internal tractions and are assumed to be either electrically impermeable or permeable. A Green's function which satisfies the conditions on the parallel edges of the strip is derived using a Fourier transform technique and applied to formulate the electroelastic crack problem in terms of a system of hypersingular integral equations. Once the hypersingular integral equations are solved, quantities of practical interest, such as the crack tip stress and electric displacement intensity factors, can be easily computed. Some specific cases of the problem are examined.

Keywords: electroelasticity, cracks, Green's function, hypersingular integral equations

This is a preprint of an article accepted for publication in the European Journal of Mechanics-A/Solids (2010).

* Author for correspondence (W. T. Ang)
E-mail: mwtang@ntu.edu.sg
http://www.ntu.edu.sg/home/mwtang/

1 Introduction

In recent years, the problem of determining the electro-elastostatic fields around cracks in an infinitely long piezoelectric strip has been a subject of considerable interest among many researchers. Most of the works reported in the literature deal with cracks that have specific geometries and orientations, such as a single straight crack oriented in a direction that is either parallel or perpendicular to the edges of the piezoelectric strip.

For mathematical simplicity, many researchers have studied cases in which the piezoelectric strip is deformed by antiplane shear stress and inplane electrical static loads. For such special cases, Li [6] and Shindo *et al* [13] applied a Fourier transform technique to reduce the problem of a straight crack to solving a Fredholm integral equation, and Li *et al* [7, 8, 19] derived closed-form formulae for the electro-elastic field intensity factors and energy release rates of a pair of collinear cracks. Some other works of related interest include those of Li and Lee [9] and Kwon and Lee [10] on a straight crack in a piezoelectric strip of finite length subject to an antiplane deformation.

If the piezoelectric strip is deformed by inplane mechanical and electrical loads, the problem is more complicated to solve. Particular plane problems involving piezoelectric strips with relatively simple crack configurations were solved by Shindo *et al* [14] and Wang *et al* [15–18].

The present paper considers the problem of an infinitely long piezoelectric strip containing an arbitrary number of arbitrarily oriented straight cracks under mixed mode electro-elastostatic loads. The cracks are assumed to be either electrically impermeable or permeable. The solution approach here is to construct an appropriate Green's function for the governing equations of linear electroelasticity and use it to reduce the problem under consideration to solving hypersingular integral equations which describe the conditions on the cracks. The Green's function which satisfies prescribed conditions on the edges of the piezoelectric strip is derived with aid of exponential Fourier transformation. Once the hypersingular integral equations are solved, physical quantities of interest such as the crack tip stress and electric displacement intensity factors can be readily computed. The analysis presented here covers both inplane and antiplane deformations and their coupling. It is applied to solve some specific cases of the problem under consideration.

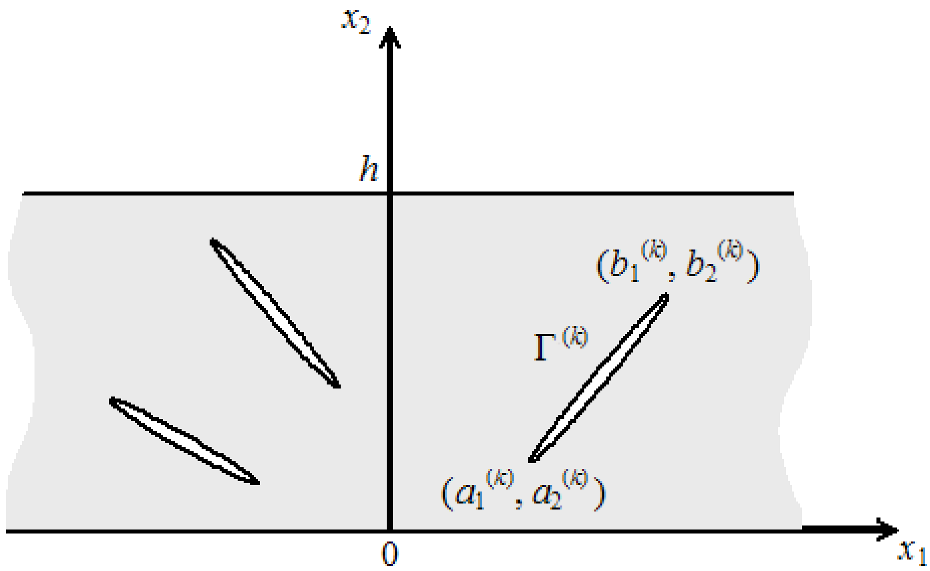

Figure 1. A sketch of the problem on the Ox_1x_2 plane.

2 The problem

With reference to an $Ox_1x_2x_3$ Cartesian coordinate system, consider an infinitely long piezoelectric strip $-\infty < x_1 < \infty$, $0 < x_2 < h$, $-\infty < x_3 < \infty$, where h is a given positive constant. The strip contains N arbitrarily oriented straight cracks whose geometries do not change along the x_3 axis. The cracks are denoted by $\Gamma^{(1)}$, $\Gamma^{(2)}$, $\cdots$, $\Gamma^{(N-1)}$ and $\Gamma^{(N)}$. On the Ox_1x_2 plane, the tips of the k-th crack $\Gamma^{(k)}$ are given by $(a_1^{(k)}, a_2^{(k)})$ and $(b_1^{(k)}, b_2^{(k)})$. Refer to Figure 1. The cracks do not intersect with one another or the edges $x_2 = 0$ and $x_2 = h$. It is also assumed that the electroelastic deformation of the cracked piezoelectric strip does not depend on the spatial coordinate x_3 and time.

We are interested in determining the displacements $u_k(x_1, x_2)$ and electric potential $\phi(x_1, x_2)$ in the cracked piezoelectric strip such that

$$\left.\begin{array}{r} \sigma_{i2}(x_1, 0) = 0 \\ d_2(x_1, 0) = 0 \\ \sigma_{i2}(x_1, h) = 0 \\ d_2(x_1, h) = 0 \end{array}\right\} \text{for } -\infty < x_1 < \infty, \tag{1}$$

$$\begin{aligned} \sigma_{ij}(x_1, x_2) m_j^{(k)} \quad \to \quad & -\sigma_{ij}^{(0)}(\xi_1, \xi_2) m_j^{(k)} \\ & \text{as } (x_1, x_2) \to (\xi_1, \xi_2) \in \Gamma_+^{(k)} (k = 1, 2, \cdots, N), \end{aligned} \tag{2}$$

and either

$$\begin{aligned} d_j(x_1, x_2) m_j^{(k)} \quad \to \quad & -d_j^{(0)}(\xi_1, \xi_2) m_j^{(k)} \\ & \text{as } (x_1, x_2) \to (\xi_1, \xi_2) \in \Gamma_+^{(k)} (k = 1, 2, \cdots, N) \\ & \text{if the cracks are electrically impermeable,} \end{aligned} \tag{3}$$

or

$$\begin{aligned} \Delta\phi(x_1, x_2) \to 0 \text{ as } (x_1, x_2) \to (\xi_1, \xi_2) \in \Gamma_+^{(k)} \text{ for } k = 1, 2, \cdots, N \\ \text{if the cracks are electrically permeable,} \end{aligned} \tag{4}$$

where σ_{ij} and d_i are respectively the stresses and electric displacements, the superscript (0) (in $\sigma_{ij}^{(0)}$ and $d_i^{(0)}$) denotes the internal stress and electric displacement fields in the piezoelectric strip, $\Gamma_+^{(k)}$ denotes the "upper face" of the crack $\Gamma^{(k)}$, $m_i^{(k)}$ being the components of a unit magnitude normal vector to $\Gamma_+^{(k)}$ which are given by

$$\begin{aligned}
m_1^{(k)} &= \frac{b_2^{(k)} - a_2^{(k)}}{\ell^{(k)}}, \ m_2^{(k)} = \frac{a_1^{(k)} - b_1^{(k)}}{\ell^{(k)}}, \ m_3^{(k)} = 0, \\
\ell^{(k)} &= \sqrt{(b_1^{(k)} - a_1^{(k)})^2 + (b_2^{(k)} - a_2^{(k)})^2},
\end{aligned} \tag{5}$$

and $\Delta\phi(x_1, x_2)$ denotes the jump in the electrical potential ϕ across opposite faces of the crack $\Gamma^{(k)}$, as defined by

$$\begin{aligned}
\Delta\phi(x_1, x_2) &= \lim_{\varepsilon \to 0}[\phi(x_1 - |\varepsilon| m_1^{(k)}, x_2 - |\varepsilon| m_2^{(k)}) \\
&\quad -\phi(x_1 + |\varepsilon| m_1^{(k)}, x_2 + |\varepsilon| m_2^{(k)})] \\
&\qquad \text{for } (x_1, x_2) \in \Gamma_+^{(k)}.
\end{aligned} \tag{6}$$

Furthermore, it is assumed that the stresses σ_{i1} and electric displacement d_1 generated by the cracks tend to zero as $|x_1| \to \infty$.

On the Ox_1x_2 plane, the crack $\Gamma^{(k)}$ may be regarded as an ellipse having a minor axis that tends to zero. If we assign a clockwise direction to the ellipse then the "upper face" $\Gamma_+^{(k)}$ is taken to be the part of the limiting ellipse from $(a_1^{(k)}, a_2^{(k)})$ to $(b_1^{(k)}, b_2^{(k)})$. For our purpose here, $\Gamma_+^{(k)}$ is treated as the straight line segment from $(a_1^{(k)}, a_2^{(k)})$ to $(b_1^{(k)}, b_2^{(k)})$.

The usual Einsteinian convention of summing over a repeated index is assumed for lowercase Latin subscripts. In general, to allow for antiplane deformations (that is, to include the case $u_3 \neq 0$), lowercase Latin subscripts take the values of 1, 2 and 3. Nevertheless, since the geometry of the problem and u_k and ϕ do not depend on x_3, some repeated lowercase subscripts may, however, run from 1 to 2 only. Thus, for example, the free subscript i in (3) and (7) below takes the values of 1, 2 and 3; the repeated subscript k in (7) may run from 1 to 3 in general; the repeated subscripts j and ℓ in (3) and (7) run from 1 to 2 only.

3 Basic equations of electroelasticity

For time independent electroelastic problems, the governing equations for the displacements u_k and electric potential ϕ in a homogeneous piezoelectric material are given by

$$
\begin{aligned}
c_{ijk\ell}\frac{\partial^2 u_k}{\partial x_j \partial x_\ell} + e_{\ell ij}\frac{\partial^2 \phi}{\partial x_j \partial x_\ell} &= 0, \\
e_{jk\ell}\frac{\partial^2 u_k}{\partial x_j \partial x_\ell} - \kappa_{j\ell}\frac{\partial^2 \phi}{\partial x_j \partial x_\ell} &= 0,
\end{aligned} \tag{7}
$$

where $c_{ijk\ell}$, $e_{\ell ij}$ and $\kappa_{i\ell}$ are the constant elastic moduli, piezoelectric coefficients and dielectric coefficients respectively.

The constitutive equations relating (σ_{ij}, d_j) and (u_k, ϕ) are

$$
\begin{aligned}
\sigma_{ij} &= c_{ijk\ell}\frac{\partial u_k}{\partial x_\ell} + e_{\ell ij}\frac{\partial \phi}{\partial x_\ell}, \\
d_j &= e_{jk\ell}\frac{\partial u_k}{\partial x_\ell} - \kappa_{jp}\frac{\partial \phi}{\partial x_\ell}.
\end{aligned} \tag{8}
$$

Following closely the approach of Barnett and Lothe [1], we define

$$
U_J = \begin{cases} u_j & \text{for } J = j = 1, 2, 3, \\ \phi & \text{for } J = 4, \end{cases}
$$

$$
S_{Ij} = \begin{cases} \sigma_{ij} & \text{for } I = i = 1, 2, 3, \\ d_j & \text{for } I = 4, \end{cases}
$$

$$
C_{IjK\ell} = \begin{cases} c_{ijk\ell} & \text{for } I = i = 1, 2, 3 \text{ and } K = k = 1, 2, 3, \\ e_{\ell ij} & \text{for } I = i = 1, 2, 3 \text{ and } K = 4, \\ e_{jk\ell} & \text{for } I = 4 \text{ and } K = k = 1, 2, 3, \\ -\kappa_{j\ell} & \text{for } I = 4 \text{ and } K = 4, \end{cases} \tag{9}
$$

so that (7) and (8) may be written more compactly as

$$
C_{IjK\ell}\frac{\partial^2 U_K}{\partial x_j \partial x_\ell} = 0 \ (I = 1, 2, 3, 4) \tag{10}
$$

and

$$S_{Ij} = C_{IjK\ell}\frac{\partial U_K}{\partial x_\ell}\ (I = 1, 2, 3, 4;\ j = 1, 2, 3) \tag{11}$$

respectively. Note that uppercase Latin subscripts have values 1, 2, 3 and 4. Summation is also implied for repeated uppercase Latin subscripts running from 1 to 4. For example, in (11) there is a summation over K from 1 to 4 and a summation over ℓ from 1 to 2.

Thus, the problem stated in Section 2 can be mathematically posed as one which requires solving (10) in the region $0 < x_2 < h$ subject to the conditions

$$\left.\begin{array}{r} S_{I2}(x_1, 0) = 0 \\ S_{I2}(x_1, h) = 0 \end{array}\right\} \text{ for } -\infty < x_1 < \infty. \tag{12}$$

$$\begin{aligned} S_{Ij}(x_1, x_2)m_j^{(k)} &\to -S_{Ij}^{(0)}(\xi_1, \xi_2)m_j^{(k)} \\ \text{as } (x_1, x_2) &\to (\xi_1, \xi_2) \in \Gamma_+^{(k)}\ (k = 1, 2, \cdots, N) \text{ for } I = 1, 2, 3, \end{aligned} \tag{13}$$

and either

$$\begin{aligned} S_{4j}(x_1, x_2)m_j^{(k)} &\to -S_{4j}^{(0)}(\xi_1, \xi_2)m_j^{(k)} \\ \text{as } (x_1, x_2) &\to (\xi_1, \xi_2) \in \Gamma_+^{(k)}\ (k = 1, 2, \cdots, N) \\ &\qquad \text{if the cracks are electrically impermeable,} \end{aligned} \tag{14}$$

or

$$\begin{aligned} &\Delta U_4(x_1, x_2) \to 0 \text{ as } (x_1, x_2) \to (\xi_1, \xi_2) \in \Gamma_+^{(k)} \text{ for } k = 1, 2, \cdots, N \\ &\qquad \text{if the cracks are electrically permeable,} \end{aligned} \tag{15}$$

where

$$\begin{aligned} \Delta U_I(x_1, x_2) &= \lim_{\varepsilon \to 0}[U_I(x_1 - |\varepsilon|m_1^{(k)}, x_2 - |\varepsilon|m_2^{(k)}) \\ &\quad - U_I(x_1 + |\varepsilon|m_1^{(k)}, x_2 + |\varepsilon|m_2^{(k)})] \\ &\qquad \text{for } (x_1, x_2) \in \Gamma_+^{(k)}. \end{aligned} \tag{16}$$

In addition, it is required that $S_{I1} \to 0$ as $|x_1| \to \infty$.

For the case in which U_K are functions of x_1 and x_2 only, the general solution of (10) can be written as

$$U_K(x_1, x_2) = \mathrm{Re}\{\sum_{\alpha=1}^{4} A_{K\alpha} f_\alpha(z_\alpha)\}, \tag{17}$$

where Re denotes the real part of a complex number, f_α are analytic functions of $z_\alpha = x_1 + \tau_\alpha x_2$ in the domain of interest, τ_α are the solutions, with positive imaginary parts, of the 8-th order polynomial (characteristic) equation

$$\det[C_{I1K1} + (C_{I1K2} + C_{I2K1})\tau + C_{I2K2}\tau^2] = 0 \tag{18}$$

and $A_{K\alpha}$ are solutions of the homogeneous system

$$[C_{I1K1} + (C_{I1K2} + C_{I2K1})\tau_\alpha + C_{I2K2}\tau_\alpha^2]A_{K\alpha} = 0. \tag{19}$$

The characteristic equation (18) admits solutions which occur in pairs of complex conjugates (Barnett and Lothe [1]).

The generalised stress functions S_{Ij} corresponding to (17) are given by

$$S_{Ij} = \mathrm{Re}\{\sum_{\alpha=1}^{4} L_{Ij\alpha} f'_\alpha(z_\alpha)\}, \tag{20}$$

where the prime denotes differentiation with respect to the relevant argument and

$$L_{Ij\alpha} = (C_{IjK1} + \tau_\alpha C_{IjK2})A_{K\alpha}. \tag{21}$$

4 Green's function for a piezoelectric strip

Here we construct a Green's function $\Phi_{KR}(x_1, x_2; \xi_1, \xi_2)$ which satisfies the partial differential equations

$$\begin{aligned} C_{IjK\ell}\frac{\partial^2}{\partial x_j \partial x_\ell}[\Phi_{KR}(x_1, x_2; \xi_1, \xi_2)] &= \delta_{IR}\delta(x_1 - \xi_1, x_2 - \xi_2) \\ \text{for } 0 &< x_2 < h \text{ and } 0 < \xi_2 < h. \end{aligned} \tag{22}$$

and the boundary conditions

$$\left.\begin{array}{l}\Xi_{I2R}(x_1,0;\xi_1,\xi_2)=0\\ \Xi_{I2R}(x_1,h;\xi_1,\xi_2)=0\end{array}\right\}\text{ for } -\infty<x_1<\infty, \tag{23}$$

where δ_{IR} is the Kronecker-delta, δ denotes the Dirac-delta function and

$$\Xi_{IjR}(x_1,x_2;\xi_1,\xi_2)=C_{IjK\ell}\frac{\partial}{\partial x_\ell}[\Phi_{KR}(x_1,x_2;\xi_1,\xi_2)]. \tag{24}$$

Guided by the analysis in Clements [3], we take

$$\begin{aligned}&\Phi_{KR}(x_1,x_2;\xi_1,\xi_2)\\ =\ &\frac{1}{2\pi}\operatorname{Re}\{\sum_{\alpha=1}^{4}A_{K\alpha}N_{\alpha S}\ln(z_\alpha-c_\alpha)\}D_{SR}+\Phi^*_{KR}(x_1,x_2;\xi_1,\xi_2)\\ &\qquad\text{for } 0<\xi_2<h,\end{aligned} \tag{25}$$

where

$$\begin{aligned}&\Phi^*_{KR}(x_1,x_2;\xi_1,\xi_2)\\ =\ &-\frac{1}{2\pi}\operatorname{Re}\{\sum_{\alpha=1}^{4}A_{K\alpha}M_{\alpha P}\sum_{\beta=1}^{4}\overline{L}_{P2\beta}\overline{N}_{\beta S}\ln(z_\alpha-\overline{c}_\beta)\}D_{SR}\\ &+\frac{1}{2\pi}\int_0^\infty\operatorname{Re}\{\sum_{\alpha=1}^{4}A_{K\alpha}M_{\alpha P}[E_{PR}(u;\xi_1,\xi_2)\exp(iuz_\alpha)\\ &\qquad-\overline{E}_{PR}(u;\xi_1,\xi_2)\exp(-iuz_\alpha)+F_{PR}(u;\xi_1,\xi_2)]\}du,\end{aligned} \tag{26}$$

the overhead bar denotes the complex conjugate of a complex number, $i=\sqrt{-1}$, $E_{PR}(u;\xi_1,\xi_2)$ and $F_{PR}(u;\xi_1,\xi_2)$ are arbitrary functions to be determined, $c_\alpha=\xi_1+\tau_\alpha\xi_2$, $[N_{\alpha S}]$ is the inverse of $[A_{K\alpha}]$, $[M_{\alpha P}]$ is the inverse of $[L_{I2\alpha}]$ and D_{SR} are real constants defined by

$$\sum_{\alpha=1}^{4}\operatorname{Im}\{L_{I2\alpha}N_{\alpha S}\}D_{SR}=\delta_{IR}. \tag{27}$$

Note that Im denotes the imaginary part of a complex number.

From (24), (25) and (26), we obtain

$$
\begin{aligned}
& \Xi_{KjR}(x_1, x_2; \xi_1, \xi_2) \\
= \; & \frac{1}{2\pi} \operatorname{Re}\{\sum_{\alpha=1}^{4} L_{Kj\alpha} N_{\alpha S} (z_\alpha - c_\alpha)^{-1}\} D_{SR} + \Xi^*_{KjR}(x_1, x_2; \xi_1, \xi_2) \\
& \qquad \text{for } 0 < \xi_2 < h, \qquad (28)
\end{aligned}
$$

where

$$
\begin{aligned}
& \Xi^*_{KjR}(x_1, x_2; \xi_1, \xi_2) \\
= \; & -\frac{1}{2\pi} \operatorname{Re}\{\sum_{\alpha=1}^{4} L_{Kj\alpha} M_{\alpha P} \sum_{\beta=1}^{4} \overline{L}_{P2\beta} \overline{N}_{\beta S} (z_\alpha - \overline{c}_\beta)^{-1}\} D_{SR} \\
& + \frac{1}{2\pi} \int_0^\infty \operatorname{Re}\{\sum_{\alpha=1}^{4} i L_{Kj\alpha} M_{\alpha P} u [E_{PR}(u; \xi_1, \xi_2) \exp(iuz_\alpha) \\
& \qquad + \overline{E}_{PR}(u; \xi_1, \xi_2) \exp(-iuz_\alpha)]\} du. \qquad (29)
\end{aligned}
$$

It can be shown that (28) and (29) satisfy (22) and the boundary conditions given on the first line in (23). The boundary conditions on the second line in (23) are fulfilled if

$$
\begin{aligned}
& \operatorname{Re}\{\sum_{\alpha=1}^{4} L_{K2\alpha} N_{\alpha S} (x_1 + \tau_\alpha h - c_\alpha)^{-1}\} D_{SR} \\
& - \operatorname{Re}\{\sum_{\alpha=1}^{4} L_{K2\alpha} M_{\alpha P} \sum_{\beta=1}^{4} \overline{L}_{P2\beta} \overline{N}_{\beta S} (x_1 + \tau_\alpha h - \overline{c}_\beta)^{-1}\} D_{SR} \\
& + \int_0^\infty \operatorname{Re}\{\sum_{\alpha=1}^{4} i L_{K2\alpha} M_{\alpha P} u [E_{PR}(u; \xi_1, \xi_2) \exp(iu[x_1 + \tau_\alpha h]) \\
& \qquad + \overline{E}_{PR}(u; \xi_1, \xi_2) \exp(-iu[x_1 + \tau_\alpha h])]\} du \\
= \; & 0 \;\; \text{for } -\infty < x_1 < \infty. \qquad (30)
\end{aligned}
$$

Taking the exponential Fourier transform of both sides of (30) over the interval $-\infty < x_1 < \infty$, we find that

$$\begin{aligned}
& u\sum_{\alpha=1}^{4}\{L_{K2\alpha}M_{\alpha P}\exp(iu\tau_\alpha h) - \overline{L}_{K2\alpha}\overline{M}_{\alpha P}\exp(iu\overline{\tau}_\alpha h)\}E_{PR}(u;\xi_1,\xi_2) \\
= & \sum_{\alpha=1}^{4}L_{K2\alpha}N_{\alpha S}\exp(-iu[c_\alpha - \tau_\alpha h])D_{SR} \\
& -\sum_{\alpha=1}^{4}L_{K2\alpha}M_{\alpha P}\sum_{\beta=1}^{4}\overline{L}_{P2\beta}\overline{N}_{\beta S}\exp(-iu[\overline{c}_\beta - \tau_\alpha h])D_{SR}. \qquad (31)
\end{aligned}$$

We can invert (31) as a system of linear algebraic equations to obtain $E_{PR}(u;\xi_1,\xi_2)$. The functions $E_{PR}(u;\xi_1,\xi_2)$ are not well defined at $u = 0$. It can be shown that the integrand of the improper integral in (26) is bounded over the interval $0 < u < \infty$ if we choose $F_{PR}(u;\xi_1,\xi_2)$ to be given by

$$F_{PR}(u;\xi_1,\xi_2) = \overline{E}_{PR}(u;\xi_1,\xi_2) - E_{PR}(u;\xi_1,\xi_2). \qquad (32)$$

Note that the functions $E_{PR}(u;\xi_1,\xi_2)$ tend to zero as the width h tends to infinity (that is, for a piezoelectric half-space $x_2 > 0$).

5 Hypersingular integral formulation

Let Ω be the region bounded by a simple closed curve $\partial\Omega$ on the Ox_1x_2 plane. If the functions $U_K(x_1,x_2)$ and $\Phi_{KR}(x_1,x_2;\xi_1,\xi_2)$ respectively satisfy (10) and (22) in Ω then it can be shown that

$$\begin{aligned}
U_R(\xi_1,\xi_2) = & \int_{\partial\Omega}[U_I(x_1,x_2)\Xi_{IjR}(x_1,x_2;\xi_1,\xi_2) \\
& -\Phi_{IR}(x_1,x_2;\xi_1,\xi_2)S_{Ij}(x_1,x_2)]n_j(x_1,x_2)ds(x_1,x_2) \\
& \text{for } (\xi_1,\xi_2)\in\Omega, \qquad (33)
\end{aligned}$$

where $[n_1(x_1,x_2), n_2(x_1,x_2)]$ is the outward unit normal to Ω at the point (x_1,x_2) on the boundary $\partial\Omega$ and $S_{Ij}(x_1,x_2)$ and $\Xi_{IjR}(x_1,x_2;\xi_1,\xi_2)$ are defined by (11) and (24) respectively. For further details on the boundary integral equations in (33), refer to Clements [3], Pan [12] and Garcia *et al* [4].

If we apply (33) together with the Green's function $\Phi_{KR}(x_1, x_2; \xi_1, \xi_2)$ and the corresponding stress function $\Xi_{KjR}(x_1, x_2; \xi_1, \xi_2)$ as given by (25), (26), (28), (29) and (31) to the crack problem stated in Section 2, we obtain

$$U_R(\xi_1, \xi_2) = \sum_{k=1}^{N} \int\limits_{\Gamma_+^{(k)}} \Delta U_I(x_1, x_2) m_p^{(k)} \Xi_{IpR}(x_1, x_2; \xi_1, \xi_2) ds(x_1, x_2) \quad \text{for } 0 < \xi_2 < h, \tag{34}$$

where $\Delta U_I(x_1, x_2)$ is as defined in (16). In (34), $\Gamma_+^{(k)}$ (the "upper face" of the crack $\Gamma^{(k)}$) is taken to be the straight line from $(a_1^{(k)}, a_2^{(k)})$ to $(b_1^{(k)}, b_2^{(k)})$.

The integration in (34) is only over the crack faces. The integrals over $x_2 = 0$ and $x_2 = h$ vanish because of (12) and (23). Also, note that the far field condition that $S_{I1} \to 0$ as $|x_1| \to 0$ is used in deriving (34).

From (11) and (34), we obtain

$$\begin{aligned} S_{Kj}(\xi_1, \xi_2) &= \sum_{k=1}^{N} \int\limits_{\Gamma_+^{(k)}} \Delta U_I(x_1, x_2) C_{KjR\ell} m_p^{(k)} \\ &\quad \times \frac{\partial}{\partial \xi_\ell} [\Xi_{IpR}(x_1, x_2; \xi_1, \xi_2)] ds(x_1, x_2) \\ &\quad \text{for } 0 < \xi_2 < h. \end{aligned} \tag{35}$$

Conditions on the cracks given by (13) and either (14) (for electrically impermeable cracks) or (15) (for electrically permeable cracks) can be used to derive a system of hypersingular integral equations containing the unknown functions $\Delta U_I(x_1, x_2)$ for $(x_1, x_2) \in \Gamma_+^{(k)}$ ($k = 1, 2, \cdots, N$). The unknown functions can be determined by solving numerically the system of hypersingular integral equations.

5.1 Electrically impermeable cracks

For electrically impermeable cracks, the system of hypersingular integral equations derived from (13) and (14) is given by

$$\mathcal{H}\int_{-1}^{+1}\frac{\chi_{IK}^{(q)}\Delta U_I^{(q)}(v)}{(t-v)^2}dv+\sum_{\substack{n=1\\n\neq q}}^{N}\int_{-1}^{+1}\Delta U_I^{(n)}(v)\Lambda_{IK}^{(nq)}(v,t)dv$$
$$+\sum_{n=1}^{N}\int_{-1}^{+1}\Delta U_I^{(n)}(v)\Psi_{IK}^{(nq)}(v,t)dv=-S_{Kj}^{(0)}(X_1^{(q)}(t),X_2^{(q)}(t))m_j^{(q)}$$
$$\text{for }-1<t<1,\ K=1,2,3,4\text{ and }q=1,2,\cdots,N\qquad,\quad(36)$$

where $\mathcal{H}$ denotes that the integral is to be interpreted in the Hadamard finite-part sense and

$$\Delta U_I^{(q)}(v)=\Delta U_I(X_1^{(q)}(v),X_2^{(q)}(v)),$$

$$\Lambda_{IK}^{(nq)}(v,t)=\frac{1}{4\pi}\operatorname{Re}\sum_{\alpha=1}^{4}\{\frac{Q_{IKrj\alpha}m_j^{(n)}m_r^{(q)}\ell^{(n)}}{([X_1^{(n)}(v)-X_1^{(q)}(t)]+\tau_\alpha[X_2^{(n)}(v)-X_2^{(q)}(t)])^2}\},$$

$$\begin{aligned}\Psi_{IK}^{(nq)}(v,t) &= \frac{m_j^{(n)}m_r^{(q)}\ell^{(n)}}{4\pi}\operatorname{Re}\{\int_0^\infty\sum_{\alpha=1}^{4}iuL_{Ij\alpha}M_{\alpha P}\\ &\times[C_{KrRs}\frac{\partial}{\partial\xi_s}(E_{PR}(u;\xi_1,\xi_2))\exp(iuZ_\alpha^{(n)}(v))\\ &+C_{KrRs}\frac{\partial}{\partial\xi_s}(\overline{E}_{PR}(u;\xi_1,\xi_2))\exp(-iuZ_\alpha^{(n)}(v))]du\\ &-\sum_{\alpha=1}^{4}L_{Ij\alpha}M_{\alpha P}\sum_{\beta=1}^{4}B_{PKr\beta}\\ &\times\frac{1}{([X_1^{(n)}(v)-X_1^{(q)}(t)]+\tau_\alpha X_2^{(n)}(v)-\overline{\tau}_\beta X_2^{(q)}(t))^2}\},\end{aligned}$$

$$
\begin{aligned}
X_1^{(q)}(v) &= \frac{(b_1^{(q)}+a_1^{(q)})}{2}+\frac{(b_1^{(q)}-a_1^{(q)})}{2}v,\\
X_2^{(q)}(v) &= \frac{(b_2^{(q)}+a_2^{(q)})}{2}+\frac{(b_2^{(q)}-a_2^{(q)})}{2}v,\\
Z_\alpha^{(q)}(v) &= X_1^{(q)}(v)+\tau_\alpha X_2^{(q)}(v),
\end{aligned}
$$

$$
\begin{aligned}
\chi_{IK}^{(q)} &= \frac{1}{\pi}\,\mathrm{Re}\sum_{\alpha=1}^{4}\{\frac{Q_{IKrj\alpha}m_j^{(q)}m_r^{(q)}\ell^{(q)}}{([b_1^{(q)}-a_1^{(q)}]+\tau_\alpha[b_2^{(q)}-a_2^{(q)}])^2}\},\\
Q_{IKrj\alpha} &= (C_{KrR1}+\tau_\alpha C_{KrR2})T_{Ij\alpha R}, \quad T_{Ij\alpha S}=L_{Ij\alpha}N_{\alpha R}D_{RS},\\
B_{PKr\beta} &= (C_{KrR1}+\overline{\tau}_\beta C_{KrR2})H_{P\beta R}, \quad H_{P\beta R}=\overline{L}_{P2\beta}\overline{N}_{\beta S}D_{SR}. \quad (37)
\end{aligned}
$$

The numerical method in Kaya and Erdogan [5] can be used to solve (36) approximately for $\Delta U_I^{(q)}(v)$ as follows.

Let

$$
\Delta U_P^{(n)}(v)\simeq\sqrt{1-v^2}\sum_{j=1}^{J}\psi_P^{(nj)}U^{(j-1)}(v), \qquad (38)
$$

where $U^{(j)}(x)=\sin([j+1]\arccos(x))/\sin(\arccos(x))$ is the j^{th} order Chebyshev polynomial of the second kind and $\psi_P^{(nj)}$ are the constants to be determined.

Substitution of (38) into (36) yields

$$
\begin{aligned}
&-\sum_{j=1}^{J} j\pi\psi_I^{(qj)}\chi_{IK}^{(q)}U^{(j-1)}(t)\\
&+\sum_{\substack{n=1\\ n\neq q}}^{N}\sum_{j=1}^{J}\psi_I^{(nj)}\int_{-1}^{+1}\sqrt{1-v^2}U^{(j-1)}(v)\Lambda_{IK}^{(nq)}(v,t)dv\\
&+\sum_{n=1}^{N}\sum_{j=1}^{J}\psi_I^{(nj)}\int_{-1}^{+1}\sqrt{1-v^2}U^{(j-1)}(v)\Psi_{IK}^{(nq)}(v,t)dv\\
=\ &-S_{Kj}^{(0)}(X_1^{(q)}(t),X_2^{(q)}(t))m_j^{(q)} \qquad (39)
\end{aligned}
$$

for $-1<t<1$, $K=1,2,3,4$ and $q=1,2,\cdots,N$.

Note that (39) contains $4JN$ unknown constants $\psi_P^{(nj)}$ ($P = 1, 2, 3, 4$; $n = 1, 2, \cdots, N$; $j = 1, 2, \cdots, J$). By letting $t = \cos([2i-1]\pi/[2J])$ for $i = 1, 2, \cdots, J$, we can generate a system of $4JN$ linear algebraic equations which can be solved for the unknown constants.

5.2 Electrically permeable cracks

From (15), $\Delta U_4^{(q)}(v) = 0$ for $-1 < v < 1$ and $q = 1, 2, \cdots, N$, if the cracks are electrically permeable. According to (13), the unknown functions $\Delta U_1^{(q)}(v)$, $\Delta U_2^{(q)}(v)$ and $\Delta U_3^{(q)}(v)$ are governed by (36) (with $\Delta U_4^{(q)}(v) = 0$) for $K = 1, 2, 3$ (instead of $K = 1, 2, 3, 4$). The functions $\Delta U_1^{(q)}(v)$, $\Delta U_2^{(q)}(v)$ and $\Delta U_3^{(q)}(v)$ can be approximated using (38) and the unknown constants $\psi_1^{(nj)}$, $\psi_2^{(nj)}$ and $\psi_3^{(nj)}$ are given by (39) with $\psi_4^{(nj)} = 0$ for $K = 1, 2, 3$ (instead of $K = 1, 2, 3, 4$). As before, we can let $t = \cos([2i-1]\pi/[2J])$ for $i = 1, 2, \cdots, J$, to generate a system of $3JN$ linear algebraic equations to solve for the unknowns.

6 Stress and electric displacement intensity factors

For the specific problems considered below in Section 7, we calculate the stress and electric displacement intensity factors at the tips $(a_1^{(n)}, a_2^{(n)})$ and $(b_1^{(n)}, b_2^{(n)})$ of the n-th crack $\Gamma^{(n)}$ defined as follows:

$$\begin{aligned}
K_I(a_1^{(n)}, a_2^{(n)}) &= \lim_{t\to -1^-} \sqrt{\frac{\ell^{(n)}}{2}}\sqrt{-2(t+1)}(S_{1j}(X_1^{(n)}(t), X_2^{(n)}(t))m_1^{(n)} \\
&\quad + S_{2j}(X_1^{(n)}(t), X_2^{(n)}(t))m_2^{(n)})m_j^{(n)}, \\
K_{II}(a_1^{(n)}, a_2^{(n)}) &= \lim_{t\to -1^-} \sqrt{\frac{\ell^{(n)}}{2}}\sqrt{-2(t+1)}(S_{1j}(X_1^{(n)}(t), X_2^{(n)}(t))m_2^{(n)} \\
&\quad - S_{2j}(X_1^{(n)}(t), X_2^{(n)}(t))m_1^{(n)})m_j^{(n)},
\end{aligned}$$

$$
\begin{aligned}
K_{III}(a_1^{(n)}, a_2^{(n)}) &= \lim_{t \to -1^-} \sqrt{\frac{\ell^{(n)}}{2}} \sqrt{-2(t+1)} S_{3j}(X_1^{(n)}(t), X_2^{(n)}(t)) m_j^{(n)}, \\
K_{IV}(a_1^{(n)}, a_2^{(n)}) &= \lim_{t \to -1^-} \sqrt{\frac{\ell^{(n)}}{2}} \sqrt{-2(t+1)} S_{4j}(X_1^{(n)}(t), X_2^{(n)}(t)) m_j^{(n)}, \\
K_I(b_1^{(n)}, b_2^{(n)}) &= \lim_{t \to 1^+} \sqrt{\frac{\ell^{(n)}}{2}} \sqrt{2(t-1)} (S_{1j}(X_1^{(n)}(t), X_2^{(n)}(t)) m_1^{(n)} \\
&\quad + S_{2j}(X_1^{(n)}(t), X_2^{(n)}(t)) m_2^{(n)}) m_j^{(n)}, \\
K_{II}(b_1^{(n)}, b_2^{(n)}) &= \lim_{t \to 1^+} \sqrt{\frac{\ell^{(n)}}{2}} \sqrt{2(t-1)} (S_{1j}(X_1^{(n)}(t), X_2^{(n)}(t)) m_2^{(n)} \\
&\quad - S_{2j}(X_1^{(n)}(t), X_2^{(n)}(t)) m_1^{(n)}) m_j^{(n)}, \\
K_{III}(b_1^{(n)}, b_2^{(n)}) &= \lim_{t \to 1^+} \sqrt{\frac{\ell^{(n)}}{2}} \sqrt{2(t-1)} S_{3j}(X_1^{(n)}(t), X_2^{(n)}(t)) m_j^{(n)}, \\
K_{IV}(b_1^{(n)}, b_2^{(n)}) &= \lim_{t \to 1^+} \sqrt{\frac{\ell^{(n)}}{2}} \sqrt{2(t-1)} S_{4j}(X_1^{(n)}(t), X_2^{(n)}(t)) m_j^{(n)}. \quad (40)
\end{aligned}
$$

Using (35) and (38), we find that (40) gives

$$
\begin{aligned}
K_I(a_1^{(n)}, a_2^{(n)}) &\simeq \sqrt{\frac{\ell^{(n)}}{2}} \pi (\chi_{P1}^{(n)} m_1^{(n)} + \chi_{P2}^{(n)} m_2^{(n)}) \sum_{j=1}^{J} \psi_P^{(nj)} U^{(j-1)}(-1) \\
K_{II}(a_1^{(n)}, a_2^{(n)}) &\simeq \sqrt{\frac{\ell^{(n)}}{2}} \pi (\chi_{P1}^{(n)} m_2^{(n)} - \chi_{P2}^{(n)} m_1^{(n)}) \sum_{j=1}^{J} \psi_P^{(nj)} U^{(j-1)}(-1), \\
K_{III}(a_1^{(n)}, a_2^{(n)}) &\simeq -\sqrt{\frac{\ell^{(n)}}{2}} \pi \chi_{P3}^{(n)} \sum_{j=1}^{J} \psi_P^{(nj)} U^{(j-1)}(-1) \\
K_{IV}(a_1^{(n)}, a_2^{(n)}) &\simeq -\sqrt{\frac{\ell^{(n)}}{2}} \pi \chi_{P4}^{(n)} \sum_{j=1}^{J} \psi_P^{(nj)} U^{(j-1)}(-1) \\
K_I(b_1^{(n)}, b_2^{(n)}) &\simeq \sqrt{\frac{\ell^{(n)}}{2}} \pi (\chi_{P1}^{(n)} m_1^{(n)} + \chi_{P2}^{(n)} m_2^{(n)}) \sum_{j=1}^{J} \psi_P^{(nj)} U^{(j-1)}(+1) \\
K_{II}(b_1^{(n)}, b_2^{(n)}) &\simeq \sqrt{\frac{\ell^{(n)}}{2}} \pi (\chi_{P1}^{(n)} m_2^{(n)} - \chi_{P2}^{(n)} m_1^{(n)}) \sum_{j=1}^{J} \psi_P^{(nj)} U^{(j-1)}(+1),
\end{aligned}
$$

$$
\begin{aligned}
K_{III}(b_1^{(n)}, b_2^{(n)}) &\simeq -\sqrt{\frac{\ell^{(n)}}{2}}\pi\chi_{P3}^{(n)}\sum_{j=1}^{J}\psi_P^{(nj)}U^{(j-1)}(+1) \\
K_{IV}(b_1^{(n)}, b_2^{(n)}) &\simeq -\sqrt{\frac{\ell^{(n)}}{2}}\pi\chi_{P4}^{(n)}\sum_{j=1}^{J}\psi_P^{(nj)}U^{(j-1)}(+1). \qquad (41)
\end{aligned}
$$

7 Specific cases

Some specific cases of the electroelastic crack problem stated in Section 2 are solved here using the analysis presented in Section 5.

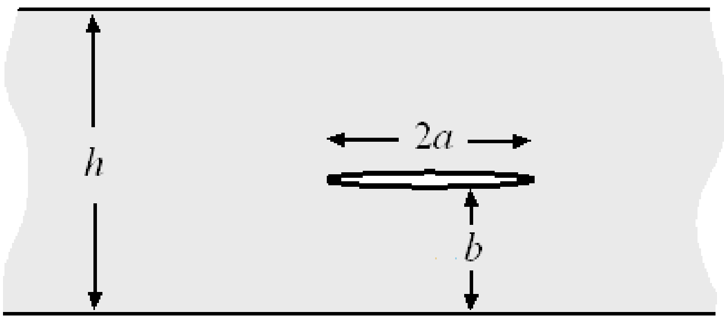

Figure 2. A horizontal electrically impermeable crack in the strip.

Case 1. To check our results against those given in Wang and Noda [18], we consider the case of a single horizontal straight crack $-a < x_1 < a$, $x_2 = b$, $-\infty < x_3 < \infty$, in the infinitely-long piezoelectric strip with electrical poling along the x_2 direction. Note that $a > 0$ and $0 < b < h$. We take the tips of the crack to be $(a_1^{(1)}, a_2^{(1)}) = (a, b)$ and $(b_1^{(1)}, b_2^{(1)}) = (-a, b)$. The crack is assumed to be electrically impermeable. A geometrical sketch of the problem is given in Figure 2. In [18], the same problem is formulated in terms of singular integral equations (that is, by using an approach equivalent to modelling the crack as a continuous distribution of dislocations).

For the electrical poling direction along the x_2 direction, the constitutive equations are given by

$$\begin{pmatrix} \sigma_{11} \\ \sigma_{22} \\ \sigma_{33} \\ \sigma_{32} \\ \sigma_{31} \\ \sigma_{12} \end{pmatrix} = \begin{pmatrix} A & F & N & 0 & 0 & 0 \\ F & C & F & 0 & 0 & 0 \\ N & F & A & 0 & 0 & 0 \\ 0 & 0 & 0 & L & 0 & 0 \\ 0 & 0 & 0 & 0 & \frac{1}{2}(A-N) & 0 \\ 0 & 0 & 0 & 0 & 0 & L \end{pmatrix} \begin{pmatrix} \gamma_{11} \\ \gamma_{22} \\ \gamma_{33} \\ 2\gamma_{32} \\ 2\gamma_{31} \\ 2\gamma_{12} \end{pmatrix} - \begin{pmatrix} 0 & e_2 & 0 \\ 0 & e_3 & 0 \\ 0 & e_2 & 0 \\ 0 & 0 & e_1 \\ 0 & 0 & 0 \\ e_1 & 0 & 0 \end{pmatrix} \begin{pmatrix} E_1 \\ E_2 \\ E_3 \end{pmatrix} \tag{42}$$

and

$$\begin{pmatrix} D_1 \\ D_2 \\ D_3 \end{pmatrix} = \begin{pmatrix} 0 & 0 & 0 & 0 & 0 & e_1 \\ e_2 & e_3 & e_2 & 0 & 0 & 0 \\ 0 & 0 & 0 & e_1 & 0 & 0 \end{pmatrix} \begin{pmatrix} \gamma_{11} \\ \gamma_{22} \\ \gamma_{33} \\ 2\gamma_{32} \\ 2\gamma_{31} \\ 2\gamma_{12} \end{pmatrix} + \begin{pmatrix} \epsilon_1 & 0 & 0 \\ 0 & \epsilon_2 & 0 \\ 0 & 0 & \epsilon_1 \end{pmatrix} \begin{pmatrix} E_1 \\ E_2 \\ E_3 \end{pmatrix}. \tag{43}$$

where $2\gamma_{kj} = \partial u_k/\partial x_j + \partial u_j/\partial x_k$ and $E_k = -\partial\phi/\partial x_k$. Note that $\gamma_{33} = 0$ and $E_3 = 0$ here since u_k and ϕ are independent of x_3.

According to (7), (8), (9), (42) and (43), the non-zero coefficients C_{IjKp} are

$$C_{1111} = C_{3333} = A,\ C_{1133} = C_{3311} = N,\ C_{2222} = C,$$

$$C_{1122} = C_{2211} = C_{2233} = C_{3322} = F,$$

$$C_{1212} = C_{2112} = C_{2121} = C_{1221} = C_{2323} = C_{3223} = C_{3232} = C_{2332} = L,$$

$$C_{1313} = C_{3113} = C_{3131} = C_{1331} = \frac{1}{2}(A-N),$$

$$
\begin{aligned}
&C_{2141}=C_{1241}=C_{3243}=C_{2343}=C_{4121}=C_{4112}=C_{4332}=C_{4323}=e_1,\\
&C_{1142}=C_{3342}=C_{4211}=C_{4233}=e_2,\\
&C_{2242}=C_{4222}=e_3,\ C_{4141}=C_{4343}=-\epsilon_1,\ C_{4242}=-\epsilon_2.
\end{aligned} \tag{44}
$$

From (19), the matrix $[A_{K\alpha}]$ can then be constructed by finding non-trivial solutions of the homogeneous systems

$$
\begin{aligned}
\left(A+L\tau_\alpha^2\right)A_{1a}+(F+L)\,\tau_\alpha A_{2\alpha}+(e_1+e_2)\,\tau_\alpha A_{4\alpha} &= 0,\\
(F+L)\,\tau_\alpha A_{1a}+\left(L+C\tau_\alpha^2\right)A_{2\alpha}+\left(e_1+e_3\tau_\alpha^2\right)A_{4\alpha} &= 0,\\
\left(\frac{1}{2}(A-N)+L\tau_\alpha^2\right)A_{3\alpha} &= 0,\\
(e_1+e_2)\,\tau_\alpha A_{1a}+\left(e_1+e_3\tau_\alpha^2\right)A_{2\alpha}+\left(-\epsilon_1-\epsilon_2\tau_\alpha^2\right)A_{4\alpha} &= 0,
\end{aligned} \tag{45}
$$

where

$$
\tau_3=i\sqrt{\frac{A-N}{2L}}\quad (A>N), \tag{46}
$$

and τ_1, τ_2 and τ_4 are solutions (with positive imaginary parts) of the sextic equation in τ given by

$$
\det\begin{pmatrix} A+L\tau^2 & (F+L)\tau & (e_1+e_2)\tau \\ (F+L)\tau & L+C\tau^2 & e_1+e_3\tau^2 \\ (e_1+e_2)\tau & e_1+e_3\tau^2 & -\epsilon_1-\epsilon_2\tau^2 \end{pmatrix}=0. \tag{47}
$$

For $\alpha=3$, a non-trivial solution of (45) which forms the third column of the matrix $[A_{K\alpha}]$ is given by

$$
\begin{pmatrix} A_{13}\\ A_{23}\\ A_{33}\\ A_{43}\end{pmatrix}=\begin{pmatrix} 0\\ 0\\ 1\\ 0\end{pmatrix}. \tag{48}
$$

For $\alpha=1$, 2 and 4, if $(A+L\tau_\alpha^2)(L+C\tau_\alpha^2)-(F+L)^2\tau_\alpha^2\neq 0$, we may take $A_{3\alpha}=0$ and $A_{4\alpha}=1$ and find $A_{1\alpha}$ and $A_{2\alpha}$ by solving

$$
\begin{aligned}
\left(A+L\tau_\alpha^2\right)A_{1a}+(F+L)\,\tau_\alpha A_{2\alpha} &= -(e_1+e_2)\,\tau_\alpha,\\
(F+L)\,\tau_\alpha A_{1a}+\left(L+C\tau_\alpha^2\right)A_{2\alpha} &= -e_1-e_3\tau_\alpha^2,
\end{aligned} \tag{49}
$$

in order to construct the first, second and fourth columns of the matrix $[A_{K\alpha}]$.

To compare our results with those in Wang and Noda [18], we use the following material constants:

$$
\begin{aligned}
&A = 12.6 \times 10^{10},\ N = 5.5 \times 10^{10},\ F = 8.41 \times 10^{10},\\
&C = 11.7 \times 10^{10},\ L = 2.3 \times 10^{10},\\
&e_1 = 17.44,\ e_2 = -6.5,\ e_3 = 23.3,\\
&\epsilon_1 = 150.3 \times 10^{-10},\ \epsilon_2 = 130.0 \times 10^{-10}.
\end{aligned} \tag{50}
$$

The values of A, N, F, C and L above are in $\mathrm{N/m^2}$, e_1, e_2 and e_3 are in $\mathrm{C/m^2}$, and ϵ_1 and ϵ_2 are in C/(Vm).

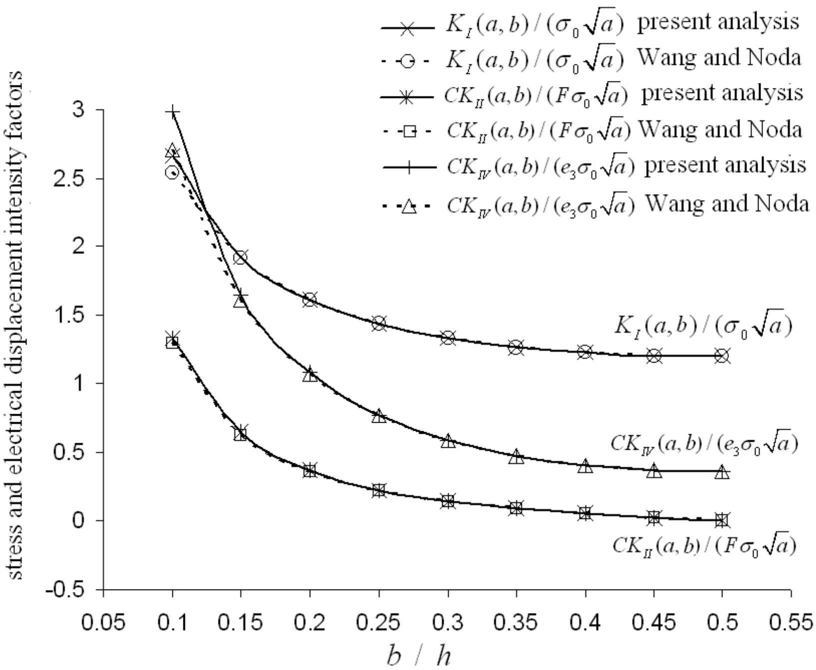

Figure 3. Plots of $K_I(a,b)/(\sigma_0\sqrt{a})$, $CK_{II}(a,b)/(F\sigma_0\sqrt{a})$ and $CK_{IV}(a,b)/(e_3\sigma_0\sqrt{a})$ against b/h.

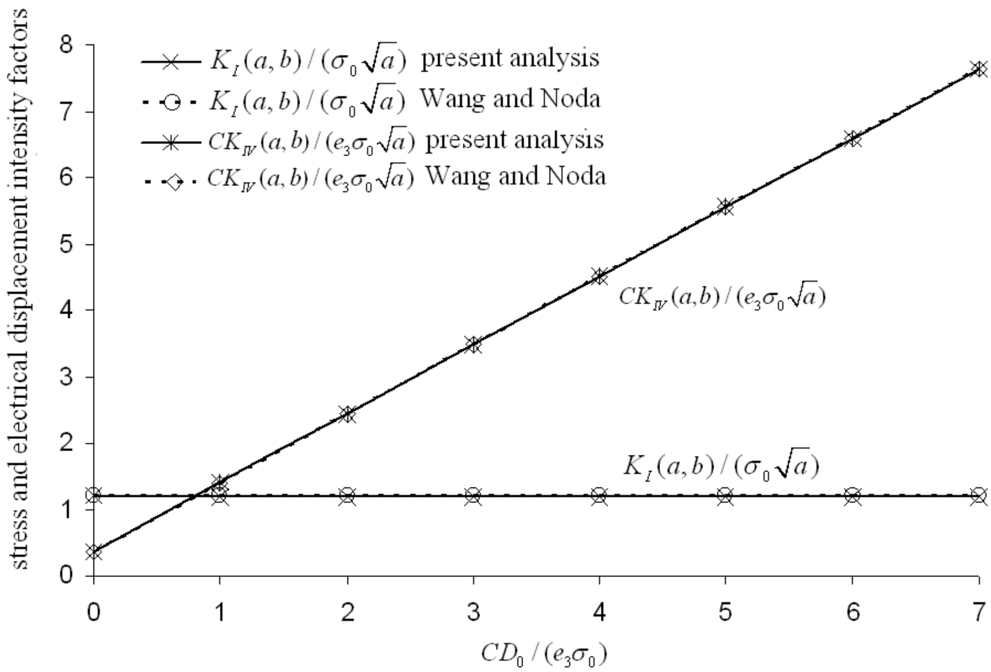

Figure 4. Plots of $K_I(a,b)/(\sigma_0\sqrt{a})$ and $CK_{IV}(a,b)/(e_3\sigma_0\sqrt{a})$ against $CD_0/(e_3\sigma_0)$.

In Figure 3, for internal loads on the crack given by $S_{12}^{(0)} = 0$, $S_{22}^{(0)} = \sigma_0$, $S_{32}^{(0)} = 0$ and $S_{42}^{(0)} = 0$ (σ_0 is a positive constant) and for $h/a = 4.0$, the non-dimensionalised crack tip stress intensity factors $K_I(a,b)/(\sigma_0\sqrt{a})$ and $CK_{II}(a,b)/(F\sigma_0\sqrt{a})$ and the non-dimensionalised crack tip electrical displacement intensity factor $CK_{IV}(a,b)/(e_3\sigma_0\sqrt{a})$ are plotted against b/h for $0.10 \leq b/h \leq 0.50$ and compared with the numerical values given by Wang and Noda in [18]. (Note that $K_{III}(a,b) = 0$ for the problem under consideration.) For $0.20 \leq b/h \leq 0.50$, our plots are almost visually indistinguishable form those obtained using the numerical values of Wang and Noda [18]. For b/h nearer to 0, there is, however, a small but noticeable difference between the two sets of values for the intensity factors. Except for b/h smaller than

0.20, the numerical values of the intensity factors are observed to converge to at least 4 significant figures when J in (38) is increased from 5 to 10. For b/h which is smaller than 0.20, that is, when there is a stronger interaction between the crack and the edge $x_2 = 0$, convergence to 2 or more significant figures is observed when we increase J from 10 to 20.

In Figure 4, for the crack under uniform internal loads $S_{12}^{(0)} = 0$, $S_{22}^{(0)} = \sigma_0$, $S_{32}^{(0)} = 0$ and $S_{42}^{(0)} = D_0$ (σ_0 is a positive constant and D_0 a non-negative constant) and for $h/a = 4.0$ and $b/h = 0.50$, we plot $K_I(a,b)/(\sigma_0\sqrt{a})$ and $CK_{IV}(a,b)/(e_3\sigma_0\sqrt{a})$ against the non-dimensionalised electrical load $CD_0/(e_3\sigma_0)$ for $0 \leq CD_0/(e_3\sigma_0) \leq 7.0$. The plots (obtained using $J = 5$ in (38)) agree well with the numerical values from Wang and Noda [18].

Case 2. Consider now the case in which the electrical poling is taken to be along the x_3 direction with the constitutive equations given by

$$\begin{pmatrix} \sigma_{11} \\ \sigma_{22} \\ \sigma_{33} \\ \sigma_{32} \\ \sigma_{31} \\ \sigma_{12} \end{pmatrix} = \begin{pmatrix} A & N & F & 0 & 0 & 0 \\ N & A & F & 0 & 0 & 0 \\ F & F & C & 0 & 0 & 0 \\ 0 & 0 & 0 & L & 0 & 0 \\ 0 & 0 & 0 & 0 & L & 0 \\ 0 & 0 & 0 & 0 & 0 & \frac{1}{2}(A-N) \end{pmatrix} \begin{pmatrix} \gamma_{11} \\ \gamma_{22} \\ \gamma_{33} \\ 2\gamma_{32} \\ 2\gamma_{31} \\ 2\gamma_{12} \end{pmatrix} - \begin{pmatrix} 0 & 0 & e_2 \\ 0 & 0 & e_2 \\ 0 & 0 & e_3 \\ 0 & e_1 & 0 \\ e_1 & 0 & 0 \\ 0 & 0 & 0 \end{pmatrix} \begin{pmatrix} E_1 \\ E_2 \\ E_3 \end{pmatrix}, \tag{51}$$

and

$$\begin{pmatrix} D_1 \\ D_2 \\ D_3 \end{pmatrix} = \begin{pmatrix} 0 & 0 & 0 & 0 & e_1 & 0 \\ 0 & 0 & 0 & e_1 & 0 & 0 \\ e_2 & e_2 & e_3 & 0 & 0 & 0 \end{pmatrix} \begin{pmatrix} \gamma_{11} \\ \gamma_{22} \\ \gamma_{33} \\ 2\gamma_{32} \\ 2\gamma_{31} \\ 2\gamma_{12} \end{pmatrix} + \begin{pmatrix} \epsilon_1 & 0 & 0 \\ 0 & \epsilon_1 & 0 \\ 0 & 0 & \epsilon_2 \end{pmatrix} \begin{pmatrix} E_1 \\ E_2 \\ E_3 \end{pmatrix}. \tag{52}$$

It follows that the non-zero coefficients C_{IjKp} are

$$\begin{aligned}
&C_{1111} = A,\ C_{2222} = A, C_{1122} = C_{2211} = N,\ C_{3333} = C, \\
&C_{1133} = C_{3311} = C_{2233} = C_{3322} = F, \\
&C_{1313} = C_{3113} = C_{3131} = C_{1331} = C_{2323} = C_{3223} = C_{3232} = C_{2332} = L, \\
&C_{1212} = C_{2112} = C_{2121} = C_{1221} = \frac{1}{2}(A-N), \\
&C_{3141} = C_{1341} = C_{2342} = C_{3242} = C_{4131} = C_{4113} = C_{4223} = C_{4232} = e_1, \\
&C_{1143} = C_{2243} = C_{4311} = C_{4322} = e_2, \\
&C_{3343} = C_{4333} = e_3,\ C_{4141} = C_{4242} = -\epsilon_1,\ C_{4343} = -\epsilon_2.
\end{aligned} \tag{53}$$

The homogeneous system in (19) reduces to

$$\begin{aligned}
(A + \frac{1}{2}(A-N)\tau_\alpha^2)A_{1\alpha} + (\frac{1}{2}N + \frac{1}{2}A)\tau_\alpha A_{2\alpha} &= 0, \\
(\frac{1}{2}N + \frac{1}{2}A)\tau_\alpha A_{1\alpha} + (\frac{1}{2}A - \frac{1}{2}N + A\tau_\alpha^2)A_{2\alpha} &= 0, \\
\left(L + L\tau_\alpha^2\right) A_{3\alpha} + \left(e_1 + e_1\tau_\alpha^2\right) A_{4\alpha} &= 0, \\
\left(e_1 + e_1\tau_\alpha^2\right) A_{3\alpha} - \left(\epsilon_1 + \epsilon_1\tau_\alpha^2\right) A_{4\alpha} &= 0.
\end{aligned} \tag{54}$$

Note that (54) cannot be used to construct $[A_{K\alpha}]$ that is invertible. To overcome this minor difficulty, a relatively small amount of anisotropy is introduced into the equations governing u_1 and u_2. Specifically, we replace

$C_{1111} = A$ in (53) by $C_{1111} = A + \varepsilon$, where ε is a selected real number whose magnitude is very small compared to A. It follows that instead of (54) the linear algebraic equations for working out $A_{K\alpha}$ are given by

$$
\begin{aligned}
(A + \varepsilon + \frac{1}{2}(A - N)\tau_\alpha^2)A_{1\alpha} + (\frac{1}{2}N + \frac{1}{2}A)\tau_\alpha A_{2\alpha} &= 0, \\
(\frac{1}{2}N + \frac{1}{2}A)\tau_\alpha A_{1\alpha} + (\frac{1}{2}A - \frac{1}{2}N + A\tau_\alpha^2)A_{2\alpha} &= 0, \\
\left(L + L\tau_\alpha^2\right) A_{3\alpha} + \left(e_1 + e_1\tau_\alpha^2\right) A_{4\alpha} &= 0, \\
\left(e_1 + e_1\tau_\alpha^2\right) A_{3\alpha} + \left(-\epsilon_1 - \epsilon_1\tau_\alpha^2\right) A_{4\alpha} &= 0.
\end{aligned} \tag{55}
$$

We can take $\tau_3 = \tau_4 = i$ and τ_1 and τ_2 are two distinct solutions with positive imaginary parts of the quartic equation

$$
\det \begin{pmatrix} A + \varepsilon + \frac{1}{2}(A - N)\tau^2 & (N + \frac{1}{2}(A - N))\tau \\ (N + \frac{1}{2}(A - N))\tau & \frac{1}{2}(A - N) + A\tau^2 \end{pmatrix} = 0. \tag{56}
$$

Note that (56) cannot yield two distinct solutions with positive imaginary parts if ε is zero.

From (55), we find that A_{Ka} may be chosen to be

$$
\begin{aligned}
A_{1\alpha} &= -\frac{(N + \frac{1}{2}(A - N))\tau_\alpha}{A + \varepsilon + \frac{1}{2}(A - N)\tau_\alpha^2}(\delta_{\alpha 1} + \delta_{\alpha 2}) \\
A_{2\alpha} &= \delta_{\alpha 1} + \delta_{\alpha 2}, \quad A_{3\alpha} = \delta_{\alpha 3}, \quad A_{4\alpha} = \delta_{\alpha 4}.
\end{aligned} \tag{57}
$$

The matrix $[A_{K\alpha}]$ as constructed in (57) is invertible if $\tau_1 \neq \tau_2$.

For electrical poling along the x_3 direction, we consider the case of two electrically permeable collinear cracks which are centrally located in the piezoelectric strip, as studied by Li [7]. Specifically, the cracks lie on the plane $x_1 = 0$ and their crack tips are given by $(a_1^{(1)}, a_2^{(1)}) = (0, h/2 - d - 2a)$, $(b_1^{(1)}, b_2^{(1)}) = (0, h/2 - d)$, $(a_1^{(2)}, a_2^{(2)}) = (0, h/2 + d)$ and $(b_1^{(2)}, b_2^{(2)}) = (0, h/2 + d + 2a)$, that is, $2a$ is the length of each of the crack and $2d$ is the distance separating the inner crack tips. A geometrical sketch of the problem is given in Figure 5. The electrically permeable cracks are acted upon by uniform internal loads given by $S_{11}^{(0)} = 0$, $S_{21}^{(0)} = 0$ and $S_{31}^{(0)} = \tau_0$ (τ_0 is a positive constant).

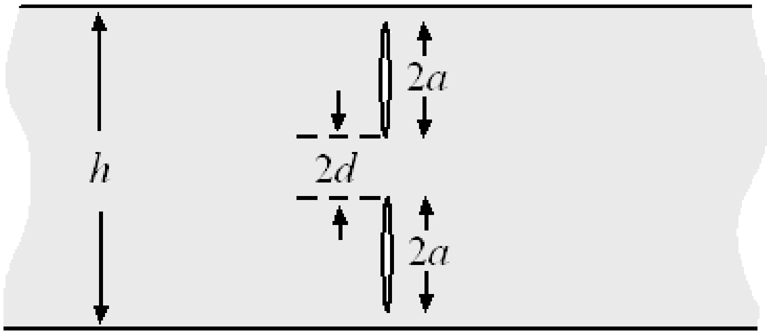

Figure 5. Two electrically permeable collinear cracks centrally located in the strip.

To obtain some numerical results, the relevant material constants are taken to be

$$\begin{aligned} &A = 12.6 \times 10^{10},\ N = 5.5 \times 10^{10},\ F = 5.3 \times 10^{10}, \\ &L = 3.53 \times 10^{10},\ e_1 = 17.0,\ \epsilon_1 = 151 \times 10^{-10}. \end{aligned} \tag{58}$$

The values of C, e_2, e_3 and ϵ_2 are not given above as they do not play a role in the computation here.

Using the constants in (58) and $J = 5$ in (38), we compute the non-dimensionalised stress intensity factors $K_{III}(0, h/2 - d - 2a)/(\tau_0\sqrt{a})$ (at an outer tip) and $K_{III}(0, h/2 - d)/(\tau_0\sqrt{a})$ (at an inner tip) for $h/a = 9$. In Figure 6, the non-dimensional stress intensity factors are plotted against d/a for $0.10 \leq d/a \leq 2.40$. The values of the stress intensity factors are in good agreement with those calculated using the analytical formulae given in Li [7].

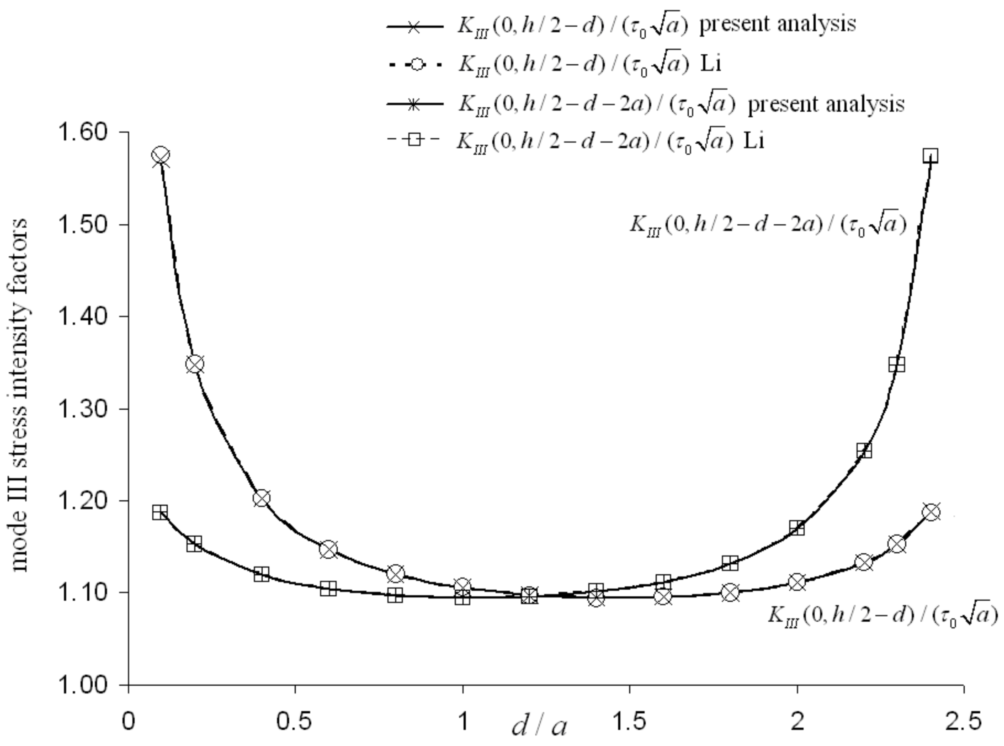

Figure 6. Plots of $K_{III}(0, h/2 - d - 2a)/(\tau_0\sqrt{a})$ and $K_{III}(0, h/2 - d)/(\tau_0\sqrt{a})$ against d/a.

Case 3. Consider now three parallel cracks in the infinitely-long piezoelectric strip as sketched in Figure 7. Specifically, the middle crack is of length $2a$ and has tips given by $(a, h/2)$ and $(-a, h/2)$. The tips of the crack above the middle crack are $(b, d + h/2)$ and $(-b, d + h/2)$ and those of the crack below are $(b, -d + h/2)$ and $(-b, -d + h/2)$. The top and bottom cracks have equal length $2b$. The uniform internal loads on the electrically impermeable cracks are given by $S_{12}^{(0)} = 0$, $S_{22}^{(0)} = \sigma_0$, $S_{32}^{(0)} = 0$ and $S_{42}^{(0)} = D_0$ with $D_0/\sigma_0 = 10^{-10}$ CN^{-1} (σ_0 and D_0 are positive constants). As in Case 1 above, the electrical poling is in the x_2 direction and the material constants of the strip are given by (50).

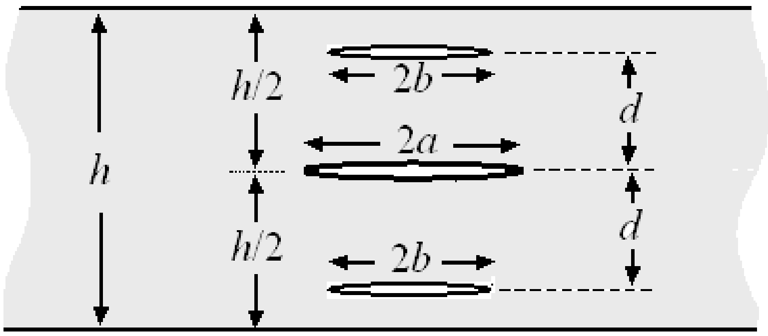

Figure 7. Three parallel cracks in the strip.

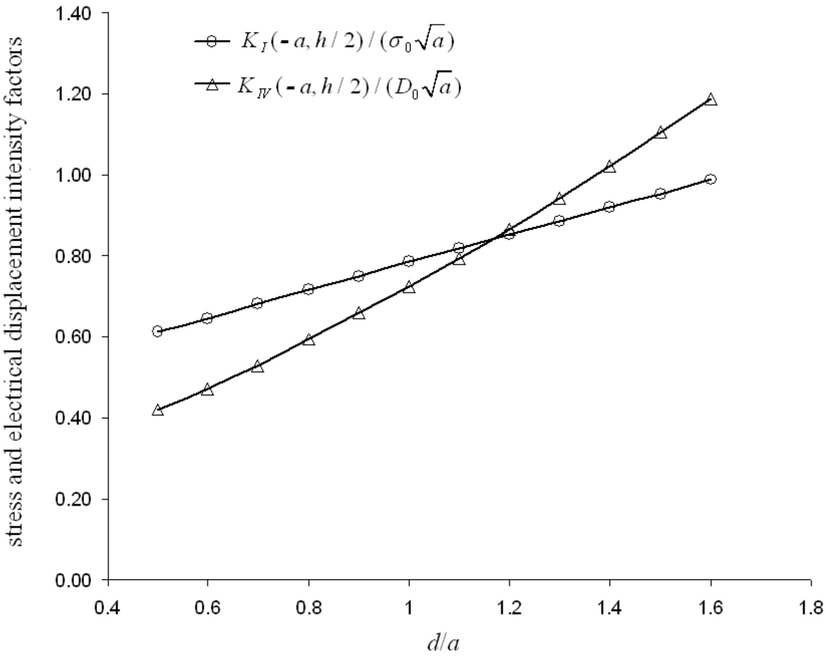

Figure 8. Plots of $K_I(-a, h/2)/(\sigma_0\sqrt{a})$ and $K_{IV}(-a, h/2)/(D_0\sqrt{a})$ against d/a.

For $h/a = 4$ and $b/a = 1$, plots of the non-dimensionalised stress intensity factor $K_I(-a, h/2)/(\sigma_0\sqrt{a})$ and the electrical displacement intensity factor $K_{IV}(-a, h/2)/(D_0\sqrt{a})$ at the tip $(-a, h/2)$ of the middle crack against d/a for $0.50 \leq d/a \leq 1.60$ are given in Figure 8.

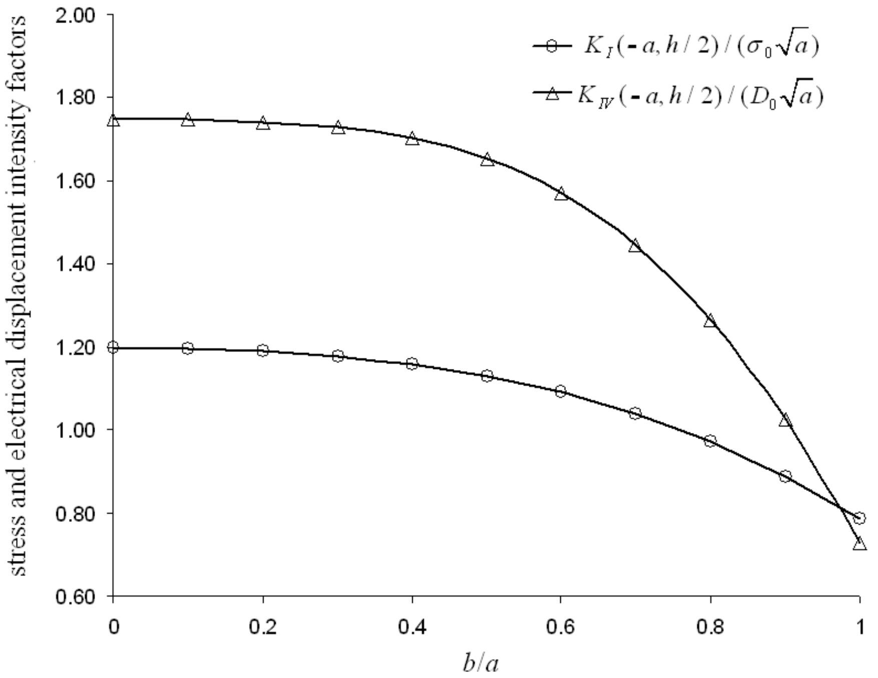

Figure 9. Plots of $K_I(-a, h/2)/(\sigma_0\sqrt{a})$ and $K_{IV}(-a, h/2)/(D_0\sqrt{a})$ against b/a.

From these plots, it may be observed that the intensity factors increase as the other two cracks move away from the middle crack. A plausible explanation for this observation may be given as follows. When the cracks are very near to one another, the stress flow lines are diverted from the tips of the middle crack, giving rise to intensity factors of lower magnitudes. As d/a increases, the stress flow lines diverted by the top and bottom cracks realign themselves perpendicularly to the planes bounding the strip, thereby interacting more strongly with the tips of the middle crack. It is clear that the top and bottom cracks have a shielding effect on the middle crack.

The shielding effect can also be observed by altering the half crack length b of the top and bottom cracks. For $h/a = 4$ and $d/a = 1$, the non-dimensionalised stress intensity factor $K_I(-a, h/2)/(\sigma_0\sqrt{a})$ and the electrical displacement intensity factor $K_{IV}(-a, h/2)/(D_0\sqrt{a})$ at the tip $(-a, h/2)$ of the middle crack are plotted against b/a for $0 \leq b/a \leq 1$ in Figure 9. It is obvious that the intensity factors decrease with increasing b/a. Their variations are quite slow and gradual as b/a increases from 0 to 0.50 and only start to become more pronounced for $b/a > 0.50$.

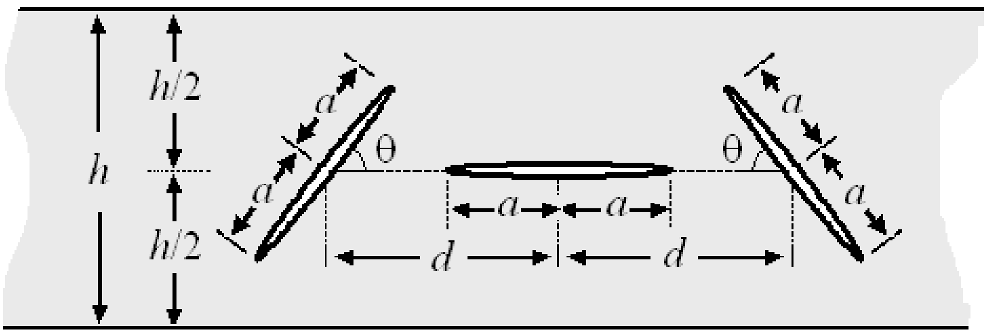

Figure 10. Two inclined cracks and a horizontal crack.

Case 4. Here we study the interaction between two inclined cracks and a horizontal crack. A geometrical sketch of the problem is given in Figure 10. Specifically, the horizontal crack lies in the region $-a < x_1 < a$, $x_2 = h/2$, $-\infty < x_3 < \infty$. The tips of the inclined crack on the left are given by $(-d + a\cos\theta, h/2 + a\sin\theta)$ and $(-d - a\cos\theta, h/2 - a\sin\theta)$ and those of the other inclined crack by $(d - a\cos\theta, h/2 + a\sin\theta)$ and $(d + a\cos\theta, h/2 - a\sin\theta)$. The uniform internal loads on the electrically impermeable cracks are given by $S_{12}^{(0)} = 0$, $S_{22}^{(0)} = \sigma_0$, $S_{32}^{(0)} = 0$ and $S_{42}^{(0)} = D_0$ with $D_0/\sigma_0 = 10^{-10}$ CN^{-1} (σ_0 and D_0 are positive constants). The electrical poling is in the x_2 direction and the material constants of the strip are given by (50).

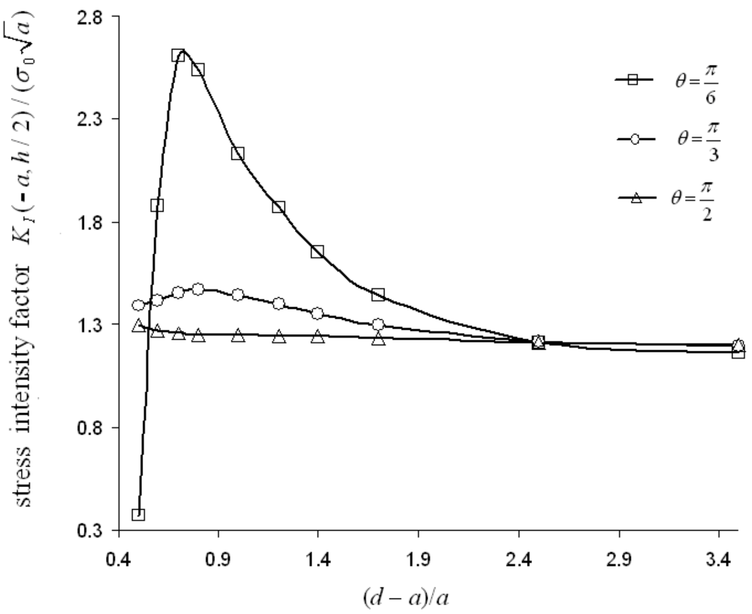

Figure 11. Plots of $K_I(-a, h/2)/(\sigma_0\sqrt{a})$ against $(d-a)/a$.

We examine the effect of the inclined cracks on the mode I stress and electrical displacement intensity factors of the horizontal crack as the distance d changes. For $h/a = 4.0$, Figures 11 and 12 give plots of $K_I(-a, h/2)/(\sigma_0\sqrt{a})$ and $K_{IV}(-a, h/2)/(D_0\sqrt{a})$ respectively against $(d-a)/a$ for $0.50 \leq (d-a)/a \leq 3.5$ for three different values of the angle θ. As expected, we observe that each of the intensity factors tends to a fixed value for all the three values of the angle θ, as the distance $(d-a)/a$ increases. For $0 \leq \theta \leq \pi/2$, the inclined cracks appear to have a greater influence on the intensity factors of the horizontal crack if the angle θ is smaller. For $\theta = \pi/6$ and $\theta = \pi/3$, each of the intensity factors has a peak value at a particular value of $(d-a)/a$. It may be of some interest to note that the variations of $K_I(-a, h/2)/(\sigma_0\sqrt{a})$ with $(d-a)/a$ are qualitatively the same as those of $K_{IV}(-a, h/2)/(D_0\sqrt{a})$.

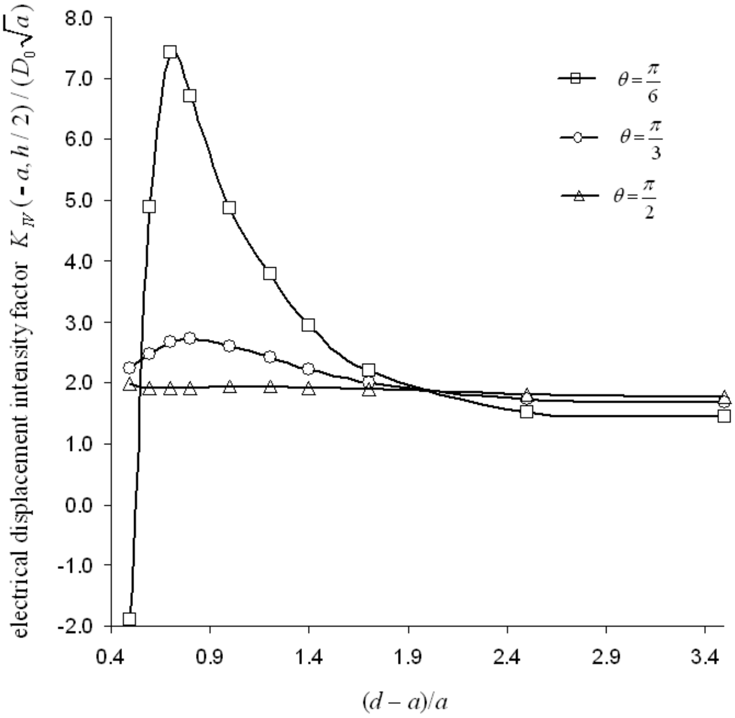

Figure 12. Plots of $K_{IV}(-a, h/2)/(D_0\sqrt{a})$ against $(d-a)/a$.

For $\theta = \pi/6$, $K_I(-a, h/2)/(\sigma_0\sqrt{a})$ is found to be negative when the non-dimensionalised distance $(d-a)/a$ is smaller than 0.50. This suggests that the inclined cracks may possibly generate a compressive load on the horizontal crack near its tips. Thus, depending on the angle θ and the distance $(d-a)/a$, opposite faces of the cracks in Figure 10 may possibly come into contact with each other near the crack tips. The solution in Section 5 assumes that the cracks open up completely under the action of suitably prescribed internal tractions and hence may not be physically valid if crack closure occurs.

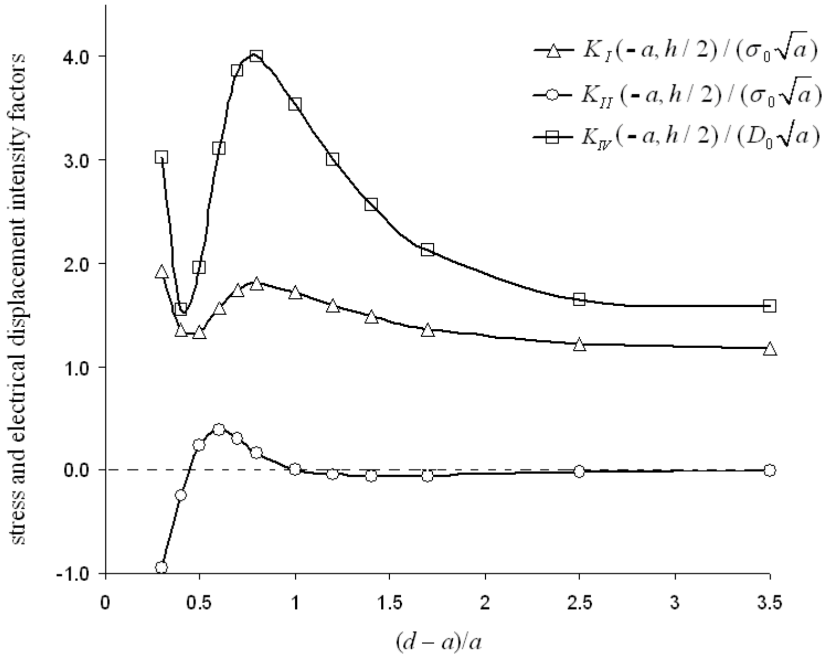

Figure 13. Plots of $K_I(-a, h/2)/(\sigma_0\sqrt{a})$, $K_{II}(-a, h/2)/(\sigma_0\sqrt{a})$ and $K_{IV}(-a, h/2)/(D_0\sqrt{a})$ against $(d-a)/a$ for $\theta = \pi/4$.

For either $(d-a)/a \to \infty$ or $\theta = \pi/2$, the mode II crack tip stress intensity factor of the horizontal crack is zero (since $S_{12}^{(0)} = 0$). In general, the presence of the inclined cracks may, however, cause a mode II deformation at the tips of the horizontal crack. In Figure 13, for $h/a = 4.0$ and $\theta = \pi/4$, the non-dimensionalised intensity factors $K_I(-a, h/2)/(\sigma_0\sqrt{a})$, $K_{II}(-a, h/2)/(\sigma_0\sqrt{a})$ and $K_{IV}(-a, h/2)/(D_0\sqrt{a})$ (at the tip $(-a, h/2)$ of the horizontal crack) are plotted against $(d-a)/a$ for $0.30 \leq (d-a)/a \leq 3.5$. Note that, as before, the variation of $K_I(-a, h/2)/(\sigma_0\sqrt{a})$ with $(d-a)/a$ shows the same qualitative feature as that of $K_{IV}(-a, h/2)/(D_0\sqrt{a})$. For $(d-a)/a \geq 1$, the mode II stress intensity factor $K_{II}(-a, h/2)/(\sigma_0\sqrt{a})$ is relatively small in magnitude. The effect of the inclined cracks on $K_{II}(-a, h/2)/(\sigma_0\sqrt{a})$ becomes more pronounced as the distance $(d-a)/a$ decreases. From Figure 13, it appears that the magnitudes of the intensity factors $K_I(-a,h/2)/(\sigma_0\sqrt{a})$, $K_{II}(-a,h/2)/(\sigma_0\sqrt{a})$ and $K_{IV}(-a,h/2)/(D_0\sqrt{a})$ increase rapidly as the crack tip $(-a,h/2)$ of the horizontal crack approaches the inclined cracks.

Case 5. Consider two centrally located parallel cracks of equal length $2a$ as sketched in Figure 14. The tips of the first crack are given by $(-d,h/2-a)$ and $(-d,h/2+a)$ and those of the second cracks by $(d,h/2-a)$ and $(d,h/2+a)$. The electrical poling is in the vertical x_2 direction. The internal tractions on the cracks are given by $S_{11}^{(0)}=\sigma_0$, $S_{21}^{(0)}=0$ and $S_{31}^{(0)}=0$. The cracks are assumed to be electrically permeable. The influence of the width h of the strip on the stress and electric displacement intensity factors at the crack tips is examined here.

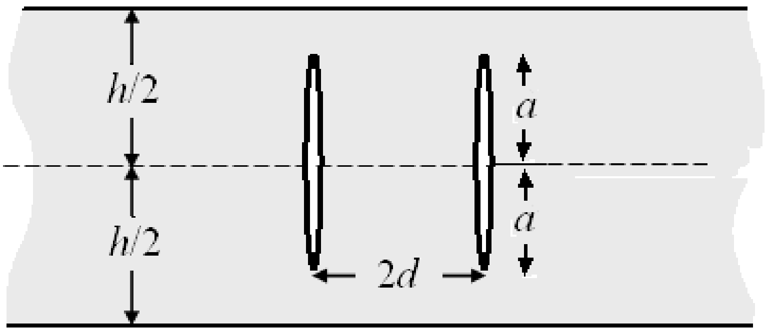

Figure 14. Two parallel cracks perpendicular to the strip.

For the case in which the material constants of the strip are given by (50), numerical values of $K_I(-d,h/2-a)/(\sigma_0\sqrt{a})$, $K_{II}(-d,h/2-a)/(\sigma_0\sqrt{a})$ and the and $CK_{IV}(-d,h/2-a)/(e_3\sigma_0\sqrt{a})$ (non-dimensionalised stress and electric displacement intensity factors at the crack tip $(-d,h/2-a)$) are given in Table 1 for $d/a=0.50$ and selected values of h/a. The numerical values of the intensity factors in Table 1 are obtained by using 10 collocation points ($J = 10$) in (38). It appears that each of the intensity factors increases in magnitude as the upper and lower planes of the strip approach the crack tips $(\pm d, h/2 + a)$ and $(\pm d, h/2 - a)$ respectively. As may be expected, the stress intensity factor K_{II} is not zero as the geometry of the problem is not symmetrical about the planes containing the cracks.

Table 1. Non-dimensionalised stress and electric displacement intensity factors on the crack tip $(-d, h/2 - a)$ for $d/a = 0.50$ and selected values of h/a.

h/a	$K_I/(\sigma_0\sqrt{a})$	$K_{II}/(\sigma_0\sqrt{a})$	$CK_{IV}/(e_3\sigma_0\sqrt{a})$
8.00	0.8092	0.1208	0.2614
6.00	0.8443	0.1234	0.2670
4.00	0.9586	0.1280	0.2770
3.50	1.0357	0.1327	0.2872
3.00	1.1933	0.1501	0.3248
2.50	1.6571	0.1991	0.4309
2.40	1.8607	0.2115	0.4577

8 Conclusion

Hypersingular integral equations are derived for an arbitrary number of arbitrarily oriented straight cracks in an infinitely long piezoelectric strip. The unknown functions in the integral equations are given by the displacement and electric potential jumps across opposite crack faces. Once the unknown functions are determined, the stress and electric displacement intensity factors at the tips of each crack can be easily computed using explicit formulae.

The hypersingular integral equations are solved for specific cases of the problem under consideration. For two of the cases, the computed values of crack tip stress and electric displacement intensity factors agree well with those published in the literature, thus verifying the validity of the solution presented here. The crack tip intensity factors for the other cases which have not been previously solved exhibit qualitative features which are physically interesting as well as intuitively acceptable.

It is possible to apply the analysis presented here to a piezoelectric strip with edge cracks if the method for solving the relevant hypersingular integral equations is appropriately modified as explained in Nied [11]. More generally, the hypersingular integral equations for curved cracks can also be derived and solved numerically as outlined in [2].

References

[1] DM Barnett and J Lothe, Dislocations and line charges in anisotropic piezoelectric insulators, *Physica Status Solidi (b)* **67** (1975) 105-111.

[2] YZ Chen, A numerical solution technique of hypersingular integral equation for curved cracks, *Communications in Numerical Methods in Engineering* **19** (2003) 645-655.

[3] DL Clements, *Boundary Value Problems Governed by Second Order Elliptic Systems*, Pitman, London, 1981.

[4] F Garcia-Sanchez, A Saez and J Dominguez, Anisotropic and piezoelectric materials fracture analysis by BEM, *Computers & Structures* **83** (2005) 804-820.

[5] AC Kaya and F Erdogan, On the solution of integral equations with strongly singular kernels, *Quarterly of Applied Mathematics* **45** (1987) 105-122.

[6] XF Li, Electroelastic analysis of an anti-plane shear crack in a piezoelectric ceramic strip, *International Journal of Solids and Structures* **39** (2002) 1097-1117.

[7] XF Li, Closed-form solution for a piezoelectric strip with two collinear cracks normal to the strip boundaries, *European Journal of Mechanics-A/Solids* **21** (2002) 981-989.

[8] XF Li and XY Duan, Closed-form solution for a mode III crack at the mid-plane of a piezoelectric layer, *Mechanics Research Communications* **28** (2001) 703-710.

[9] XF Li and KY Lee, Electroelastic behavior of a rectangular piezoelectric ceramic with an antiplane shear crack at arbitrary position, *European Journal of Mechanics-A/Solids* **23** (2004) 645-658.

[10] SM Kwon and KY Lee, Analysis of stress and electric fields in a rectangular piezoelectric body with a center crack under anti-plane shear loading, *International Journal of Solids and Structures* **37** (2000) 4859-4869.

[11] HF Nied, Periodic array of cracks in a half-plane subjected to arbitrary loading, *ASME Journal of Applied. Mechanics* **54** (1987) 642-648.

[12] E Pan, A BEM analysis of fracture mechanics in 2D anisotropic piezoelectric solids, *Engineering Analysis with Boundary Elements* **23** (1999) 67-76.

[13] Y Shindo, F Narita and K Tanaka, Electroelastic intensification near anti-plane shear crack in orthotropic piezoelectric ceramic strip, *Theoretical and Applied Fracture Mechanics* **25** (1996) 65-71.

[14] Y Shindo, K Watanabe and F Narita, Electroelastic analysis of a piezoelectric ceramic strip with a central crack, *International Journal of Engineering Science* **38** (2000) 1-19.

[15] BL Wang and Mai YW, A piezoelectric material strip with a crack perpendicular to its boundary surfaces, *International Journal of Solids and Structures* **39** (2002) 4501-4524.

[16] BL Wang and JC Han, Fracture of a finite piezoelectric strip with a crack vertical to its borders-an exact analysis and applications, *International Journal of Applied Electromagnetics and Mechanics* **27** (2007) 87-99.

[17] BL Wang, JC Han and SY Du, New considerations for the fracture of piezoelectric materials under electromechanical loading, *Mechanics Research Communications* **27** (2000) 435-444.

[18] BL Wang and N Noda, Mixed mode crack initiation in piezoelectric ceramic strip, *Theoretical and Applied Fracture Mechanics* **34** (2000) 35-47.

[19] XC Zhong and XF Li, Closed-form solution for two collinear cracks in a piezoelectric strip, *Mechanics Research Communications* **32** (2005) 401-410.